The EMBO Journal vol.15 no.2 pp.351–362, 1996

The two PAR leucine zipper proteins, TEF and DBP, display similar circadian and tissue-specific expression, but have different target promoter preferences

Philippe Fonjallaz, Vincent Ossipow, Gerhard Wanner[1] and Ueli Schibler[2]

Département de Biologie Moléculaire, Sciences II, Université de Genève, 30, quai Ernest Ansermet, and [1]Section de Mathématiques, Université de Genève, 2–4, rue du Lièvre, CH-1211 Genève-4, Switzerland

[2]Corresponding author

The two highly related PAR basic region leucine zipper proteins TEF and DBP accumulate according to a robust circadian rhythm in liver and kidney. In liver nuclei, the amplitude of daily oscillation has been estimated to be 50-fold and 160-fold for TEF and DBP, respectively. While DBP mRNA expression is the principal determinant of circadian DBP accumulation, the amplitude of TEF mRNA cycling is insufficient to explain circadian TEF fluctuation. Conceivably, daily variations in TEF degradation or nuclear translocation efficiency may explain the discrepancy between mRNA and protein accumulation. *In vitro*, TEF and DBP bind the same DNA sequences. Yet, in co-transfection experiments, these two proteins exhibit different activation potentials for two reporter genes examined. While TEF stimulates transcription from the albumin promoter more potently than DBP, only DBP is capable of activating transcription efficiently from the cholesterol 7α hydroxylase (C7αH) promoter. However, a TEF–DBP fusion protein, carrying N-terminal TEF sequences and the DNA binding/dimerization domain of DBP, enhances expression of the C7αH–CAT reporter gene as strongly as wild-type DBP. Our results suggest that the promoter environment, rather than the affinity with which PAR proteins recognize their cognate DNA sequences *in vitro*, determines the promoter preferences of TEF and DBP.

Keywords: circadian rhythm/DBP/liver/TEF/transcription factors

Introduction

The PAR family of basic region leucine zipper (bZip) proteins includes three members of mammalian origin, DBP (albumin site D-binding protein; Mueller *et al.*, 1990), TEF (thyrotroph embryonic factor; Drolet *et al.*, 1991) and HLF (hepatocyte leukemia factor; Hunger *et al.*, 1992, 1994; Inaba *et al.*, 1992, 1994). VBP (vitellogenin promoter-binding protein; Iyer *et al.*, 1991; Burch and Davis, 1994), a chicken PAR bZip protein, is highly related to TEF and is thus likely to represent the TEF ortholog in birds. All PAR bZip proteins share extensive sequence similarity (65–73%) within their C-terminal moieties, encompassing the basic zipper region required for DNA binding and dimerization, and a peptide segment called PAR (Drolet *et al.*, 1991), rich in prolines and acidic amino acids. Unlike the C-terminal moieties, the majority of N-terminal amino acid sequences show considerably less similarity (26–39%) between the three PAR family members (for review, see Lavery and Schibler, 1994). Yet, between rat and man, the entire protein sequence of all PAR family members is well conserved. In fact, the sequence identity between these two mammalian species is 98.5% for TEF, 97% for HLF and 92.3% for DBP. The extraordinary evolutionary conservation of sequences that diverge between the three PAR protein isoforms suggests that each PAR protein has at least some distinct functions.

Consistent with their highly conserved DNA binding domain (for review, see Lavery and Schibler, 1994), PAR proteins exhibit the same DNA binding specificity *in vitro* and recognize the sequence RTTAYGTAAY (R = purines, Y = pyrimidines), or slight permutations thereof (Haas *et al.*, 1995; Falvey, Marcacci and Schibler, in preparation). All PAR recognition sequences are also avidly bound by members of the C/EBP family of bZip proteins. However, the converse is not true. In fact, C/EBP proteins display a much more promiscuous DNA binding specificity than PAR proteins (Falvey, Marcacci and Schibler, in preparation). In further contrast to C/EBP isoforms (Cao *et al.*, 1991), different PAR family members homo- and heterodimerize with different efficiencies. As suggested by subunit exchange experiments, TEF homodimers and TEF–DBP heterodimers are more stable than DBP homodimers (P.Fonjallaz and U.Schibler, unpublished results). Conceivably, this may result from the different TEF and DBP leucine zipper heptad repeats ILLL and ILLV, respectively.

TEF mRNA was detected originally in early thyrotrophs of the rat pituitary gland (Drolet *et al.*, 1991). However, the expression pattern of TEF protein has not yet been reported. Since the expression of DBP, the founding member of the PAR family, follows a stringent circadian rhythm in liver, we were particularly interested in determining whether TEF expression also oscillates during the day and, thus, whether circadian expression is shared by different PAR proteins. Moreover, we wished to examine whether DBP and TEF may be functionally redundant with regard to target gene activation, given their indistinguishable DNA binding specificity *in vitro*. Here, we show that, in adult rats, the expression patterns of TEF and DBP are similar with regard to both circadian accumulation and tissue distribution. However, in contrast to circadian DBP expression, the daily amplitude of TEF is determined largely by a post-transcriptional mechanism(s). Interestingly, DBP and TEF show different activation potentials for the promoters of the two putative DBP target genes, albumin and cholesterol 7α hydroxylase (C7αH) (Mueller *et al.*, 1990; Lavery and Schibler 1993). Surprisingly,

these functional differences are accounted for mainly by the conserved bZip regions of these two proteins, rather than the more diverse N-terminal sequences.

Results

TEF expression is strongly circadian in liver nuclei

DBP, the founding member of the PAR family, has been demonstrated to accumulate according to a stringent circadian rhythm in parenchymal hepatocytes of rats entrained at a 12 h dark–light cycle (6 a.m. lights on, 6 p.m., lights off; Wuarin and Schibler, 1990). Highest protein levels were observed at 8 p.m., at which time this protein reaches close to micromolar concentrations in liver nuclei (F.Fleury-Olela and U.Schibler, unpublished). In order to examine whether TEF and DBP are co-expressed in liver and, if so, whether the accumulation of both of these proteins oscillates during the day, nuclear extracts were probed by Western blot analysis with rabbit antisera raised against TEF and DBP recombinant proteins, respectively. Unfractionated DBP and TEF immune sera recognized both of these proteins, with only a 2- to 3-fold preference for the antigen against which they were raised. As both TEF and DBP migrate with apparent molecular weights between 45 and 47 kDa on SDS–polyacrylamide gels, this moderate immunological specificity did not allow discrimination between these related proteins. More specific TEF and DBP antibodies were obtained by immunodepletion of cross-reactive antibodies from the respective sera, and by affinity purification of the remaining epitope-specific antibodies (see Materials and methods). Extracts were prepared from liver nuclei harvested at 4 h intervals around the clock and fractionated by SDS–PAGE along with, as control, an equimolar mixture of recombinant TEF and DBP. Immunoblot analysis of these nuclear proteins with affinity-purified TEF and DBP antibodies revealed a strong circadian accumulation for both proteins (Figure 1A). In several independent experiments, peak accumulation has been observed at 8 p.m. for TEF and DBP. Thus, both the period and the phase of circadian TEF and DBP accumulation appear to be highly similar. As seen in the control with *Escherichia coli*-derived recombinant proteins (Figure 1A, lane 'rec'), the affinity-purified TEF and DBP antibodies recognize exclusively their respective epitopes. Moreover, as the signals for the recombinant proteins are similar for DBP and TEF antibodies, the TEF and DBP signals obtained with the liver extracts can be compared directly. Thus, it appears that TEF reaches an ~3-fold lower concentration than DBP in liver nuclei. The signals observed in immunoblots using the ECL system were quantified by laser scanning, and suggested daily amplitudes of >100-fold for both TEF and DBP. To determine the amplitude of TEF and DBP oscillation more precisely, we performed serial dilution experiments (Figure 1B). Decreasing amounts of evening (8 p.m.) nuclear extracts were diluted with morning (8 a.m.) extracts, and the resulting protein mixtures were again subjected to a Western blot analysis. The amplitude can be estimated fairly accurately in this experiment, since those mixtures which were used for quantification were those in which morning and evening extracts contribute similarly to the immunoblot signal for TEF and DBP. As shown in Figure 1B, the evening extract

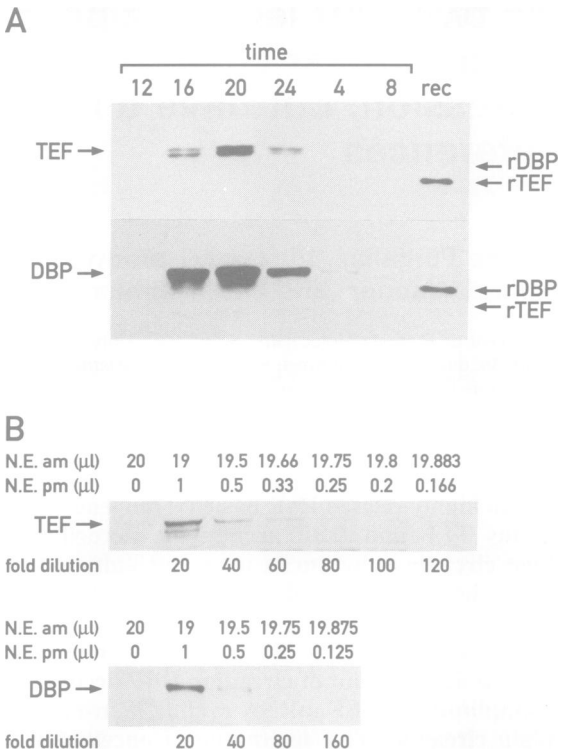

Fig. 1. Circadian accumulation of TEF and DBP proteins. (**A**) Western blot analysis of rat liver nuclear proteins (25 µg) harvested at 4 h intervals during 24 h, as indicated above each lane. Lane 'rec' contains equimolar amounts of recombinant TEF and DBP protein, in order to control for the antibody specificity. The positions of recombinants (rDBP, rTEF) and rat liver proteins (DBP, TEF) are indicated at the right and left, respectively. (**B**) Western blot analysis to estimate the amplitude of circadian TEF and DBP protein accumulation. Morning (8 a.m.) and evening (8 p.m.) nuclear extracts were mixed as indicated above the figure and subjected to immunoblot analysis with monospecific TEF and DBP antibodies (the protein concentration was 12.5 mg/ml for both morning and evening extracts). Fold dilutions of the 8 p.m. extract are depicted under each lane.

had to be diluted ~50-fold and 160-fold with morning extract for TEF and DBP, respectively, in order to yield an ~2-fold higher signal than the one observed with morning extracts alone. Thus, TEF and DBP levels oscillate with an amplitude of ~50-fold and 160-fold, respectively, during the day.

In conclusion, the data presented in this section suggest that the two PAR bZip proteins, TEF and DBP, accumulate with a robust circadian amplitude in liver nuclei. Moreover, the phase angles of these oscillation are highly similar, opening up the possibility that expression of both TEF and DBP is regulated coordinately.

TEF mRNA expression oscillates with a lower amplitude than TEF protein

Circadian expression of DBP has been suggested to be regulated mainly at the level of mRNA accumulation, which in turn appears to be controlled by circadian transcription (Wuarin and Schibler, 1990, 1994). We wished to examine whether cyclic TEF expression, like DBP expression, can also be accounted for by circadian mRNA accumulation. Therefore, an RNase mapping experiment with TEF and DBP antisense RNA probes was performed with whole cell liver RNA harvested at 4 h

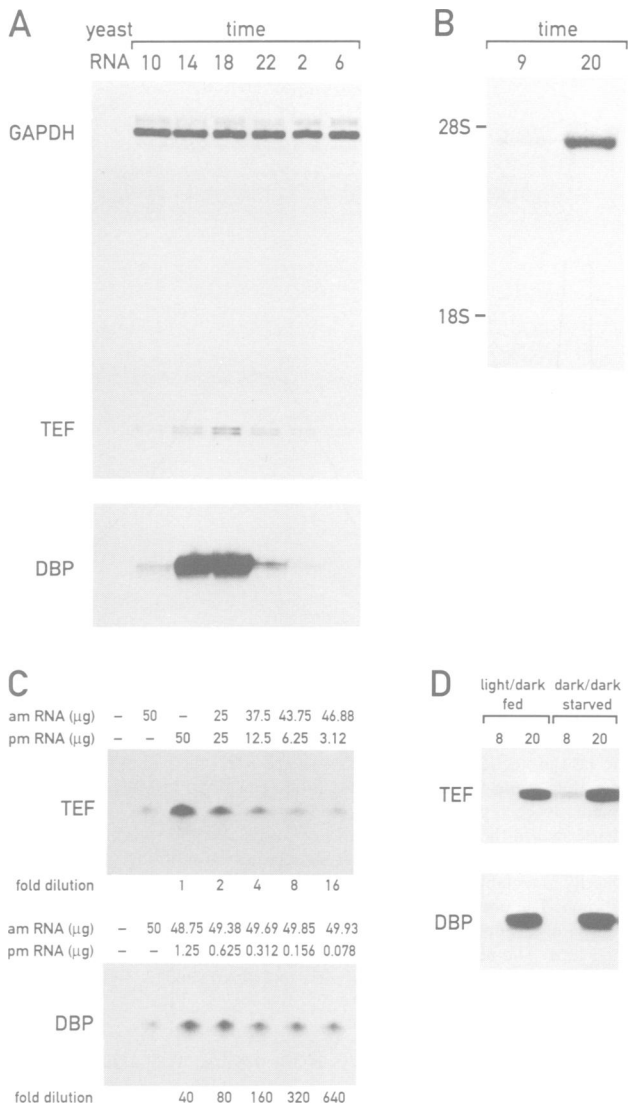

Fig. 2. Circadian accumulation of TEF and DBP mRNA. (**A**) RNase protection analysis of whole cell RNA (50 µg) isolated from rat liver at 4 h intervals during 24 h, as indicated above each lane, with TEF, DBP and GAPDH RNA antisense RNA probes (see Materials and methods). Yeast RNA was included as a negative control. Note that the levels of GADPH transcripts remain constant throughout the day. (**B**) Northern blot analysis of rat liver poly(A)$^+$ RNA (10 µg) harvested at 9 or 20 h. The same radiolabeled TEF antisense RNA probe was used as in the RNase protection experiments. The positions of rRNA species are shown at the left. (**C**) RNase protection analysis to measure the amplitude of circadian TEF and DBP mRNA accumulation. Morning (6 a.m.) and evening (6 p.m.) whole cell RNAs were mixed as indicated above each lane and subjected to RNase protection assays using the same RNA probes as in (A). Fold dilutions of the evening extracts are depicted under each lane. (**D**) RNase protection analysis of whole cell liver RNA from rats that, after circadian entrainment at 12 h light–dark cycles (6 a.m. lights on, 6 p.m. lights off) for several weeks, were kept in constant dark for 7 days. In addition, the animals were starved for 2 days before being sacrificed. As a control, the same analysis was performed on animals that were kept under continuous 12 h light–dark cycles (6 a.m. lights on, 6 p.m. lights off), and that were fed *ad libitum*.

intervals around the clock (Figure 2A). A glyceraldehyde phosphate dehydrogenase (GAPDH) antisense RNA probe (Schmidt and Schibler, 1995a) was included in these RNase protection experiments as an internal control for a transcript that accumulates at constant levels throughout the day. In agreement with previously reported experiments (Wuarin and Schibler, 1990), DBP mRNA levels vary dramatically during the day, with maximum and minimum levels observed at 6 p.m. and 6 a.m., respectively. A serial dilution experiment, conceptually similar to the one described for TEF and DBP proteins, revealed an amplitude of ~200- to 400-fold for DBP mRNA (Figure 2C, lower panel). In contrast, TEF mRNA levels vary only ~5- to 10-fold between the evening and the morning (Figure 2B and C). A similar amplitude (8-fold) was also observed in a Northern blot analysis, which revealed a single TEF mRNA band migrating close to the 28S rRNA (Figure 2B). The daily oscillations of TEF and DBP mRNA accumulation can be considered as true circadian rhythms, since they persist in animals that were kept for 1 week in constant dark and that were starved for 2 days before they were sacrificed (Figure 2D).

In the simplest scenario, circadian TEF and DBP mRNA accumulation alone would account for the observed circadian TEF and DBP expression in liver nuclei. If this were the case, the following parameters contributing to the nuclear accumulation of DBP and TEF should be constant throughout the day: (i) translation rate per mRNA; (ii) nuclear translocation efficiency; and (iii) protein half-life. The following differential equation describes the relationship between protein and mRNA accumulation for such a simple model (Wuarin *et al.*, 1992):

$$[P](x) = C \cdot \int_{-\infty}^{x} e^{\ln 2(t-x)/t_{1/2}} \cdot f(t)[\text{mRNA}] \cdot dt \qquad (1)$$

Where [P] is the protein concentration, x the time of accumulation, $t_{1/2}$ the protein half-life (assuming first order kinetics for degradation), $f(t)$[mRNA] the function of time (t) of mRNA accumulation (which is, in this model, proportional to the protein synthesis function), and C a constant depending on the absolute values for the translation rate and the cellular mRNA concentration. By applying this simple model for both TEF and DBP, we attempted to simulate TEF and DBP protein accumulation, using the 'best fit function' (see Materials and methods) for the experimentally determined mRNA values (Figure 3A and B) as the time-dependent function of mRNA accumulation. As shown in Figure 3C, such a model is adequate to explain the circadian DBP protein accumulation profile. Indeed, the simulated curve closely matches the experimentally determined protein data points (see legend to Figure 3 for statistical significance) and suggests that DBP decays with a constant half-life of 2.2 h. For TEF, however, the above model is inappropriate to simulate the circadian TEF protein accumulation profile. As shown in Figure 3D, the best simulated TEF accumulation curve does not fit the experimentally determined protein accumulation data points. Thus, one or more of the three parameters: (i) translation rate per mRNA; (ii) nuclear translocation efficiency and (iii) protein half-life, must vary during the day, in addition to the cellular mRNA concentration. The kinetic determination of any one of these parameters would be a nearly impossible endeavor, given the relatively low abundance of TEF, the oscillating TEF synthesis and the difficulty in keeping pools of radiolabeled amino acids constant in the intact animal. However, the translatability

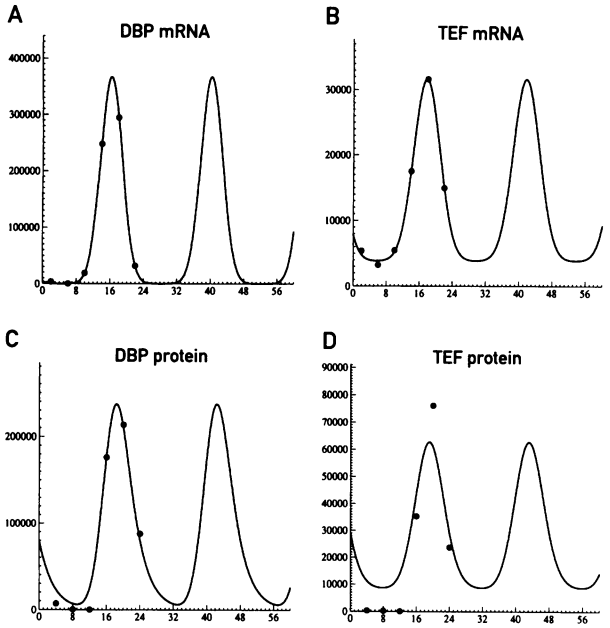

Fig. 3. Mathematical simulation of TEF and DBP protein accumulation. (**A**) Best fit Gaussian-type periodic function for DBP mRNA accumulation. Filled circles represent the experimental data points. (**B**) Best fit Gaussian-type periodic function for TEF mRNA accumulation. Filled circles represent the experimental data points. (**C**) Simulation of DBP protein accumulation using the differential equation 1 described in the text and the curve calculated in (A) as the function of mRNA accumulation, which is assumed to be proportional to the protein synthesis function (see text). Filled circles represent the experimental data points. The experimentally determined DBP protein cycle matches the accumulation curve predicted for a protein with a half-life of 2.2 h with a good statistical significance ($t_{1/2}$ = 2.2, C = 0.277, χ^2 sum = 9, degrees of freedom = 4). (**D**) Simulation of TEF protein accumulation using the differential equation 1 described in the text and the curve calculated in (B) as the function of mRNA accumulation. The best simulated TEF protein accumulation curve shown here ($t_{1/2}$ = 1.02, C = 1.45, χ^2 sum = 81, degrees of freedom = 4) does not fit the experimental data points with a reasonable statistical significance (see χ^2 sum).

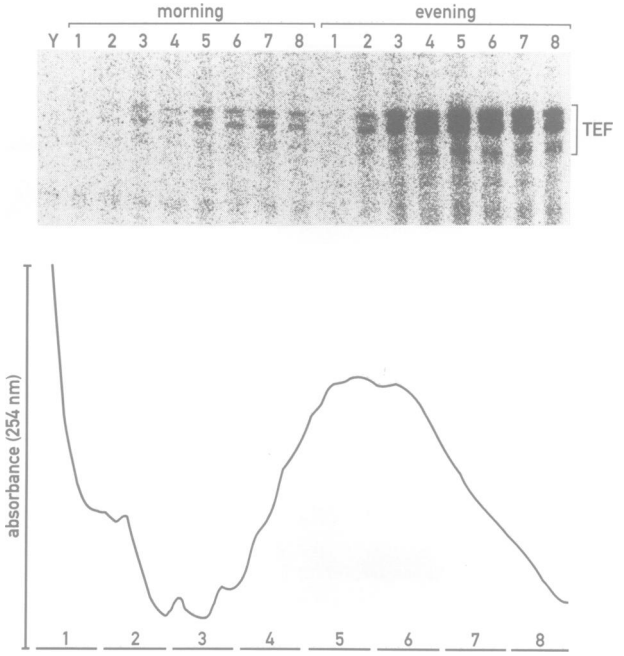

Fig. 4. Polysomal distribution of TEF mRNA. Polysomes from 250 mg of liver tissue were separated into eight fractions by velocity sedimentation through sucrose gradients. The top panel shows the RNase protection analysis of 25% of the RNA recovered from each fraction, using the TEF antisense probe described in Materials and methods. Two parallel sucrose gradients using rat liver cytoplasm harvested in the morning (8 a.m.) or in the evening (8 p.m.) were analyzed. Since the TEF mRNA signals for the morning sample are hardly detectable by autoradiography, PhosphorImager scans are shown. The bottom panel shows the absorbance scan (OD_{254}, arbitrary units) of a representative sucrose gradient; fraction 1 is from the top of the tube. The absorbance profiles for polysomes harvested during the morning or during the evening were indistinguishable.

of TEF mRNA may be reflected in its association with ribosomes. We thus resorted to an indirect technique to evaluate whether the translation efficiency of TEF mRNA may fluctuate during the day. To this end, cytoplasmic extracts were prepared at 8 p.m. and 8 a.m., and the polyribosomes were fractionated according to their sizes (number of ribosomes) by velocity sedimentation through sucrose gradients. RNA was extracted from each fraction and examined by RNase mapping for the presence of TEF mRNA. Figure 4 demonstrates that, during morning and evening, the distribution profiles of TEF mRNA across the sucrose gradient are similar, indicating that TEF mRNA is loaded with a similar number of ribosomes throughout the day. This suggests that the translation efficiency of TEF mRNA does not vary dramatically during the day. We thus suspect that either TEF degradation or nuclear translocation may fluctuate in addition to TEF mRNA accumulation, thereby amplifying cyclic TEF protein expression in liver nuclei.

TEF and DBP show similar tissue distributions

In the previous section, we have demonstrated that TEF and DBP are co-expressed in the liver. To examine the tissue distribution of these two proteins further, whole cell RNAs and nuclear extracts from a variety of tissues (liver, brain, kidney, spleen, testis and lung) were subjected to RNase protection experiments and immunoblot analysis, respectively. For each tissue, RNA and nuclear proteins were harvested at times when their accumulation is either maximal or minimal in liver. Figure 5A shows that TEF and DBP mRNA can be detected in all of the examined tissues. In liver, kidney, spleen and lung, the levels of both mRNAs undergo circadian variation. In brain, which contains both mRNAs at relatively high levels, TEF mRNA is expressed constitutively, and DBP mRNA varies only ~3-fold during the day. Testis contains low amounts of both DBP and TEF mRNA. Figure 5B displays the tissue-specific accumulation of TEF and DBP, as measured by immunoblotting with affinity-purified antibodies. Both proteins exhibit a stringent circadian accumulation in liver and kidney, both proteins oscillate with a low amplitude in brain, and both proteins are virtually absent from spleen and testis. In contrast, DBP also displays circadian accumulation in lung, a tissue in which TEF is hardly detectable.

A comparison of Figure 5A and B may lead to the conclusion that there is a striking discrepancy between the spatial expression patterns of mRNA and protein for both TEF and DBP. However, these differences are diminished considerably when the mRNA signals are corrected for cell size (see Figure 5C and Discussion). A

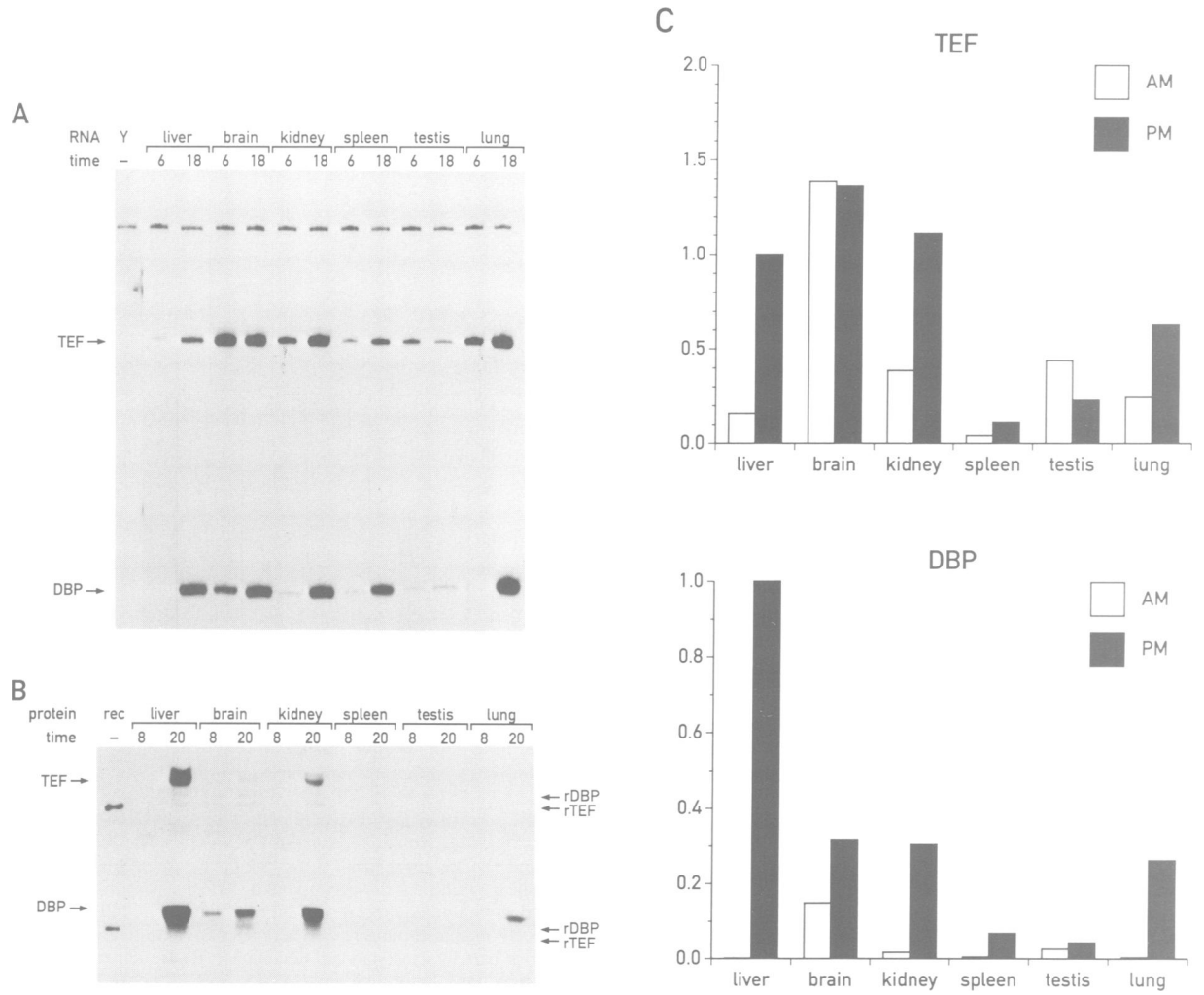

Fig. 5. Tissue-specific accumulation of TEF and DBP mRNAs and proteins. (**A**) RNase protection analysis of whole cell RNAs (50 μg) from six rat tissues, as indicated above each lane, harvested at 6 a.m. (6) or 6 p.m. (18). Lane Y contains yeast RNA (negative control). Positions of protected fragments are indicated at the left. In order to estimate the cellular mRNA levels, the signals observed in the RNase protection assays have to be corrected for the tissue-specific RNA:DNA ratios (see C). (**B**) Western blot analysis of rat nuclear extracts from six different tissues, as indicated above each lane, harvested at 8 a.m. (8) or 8 p.m. (20), and probed with TEF or DBP monospecific antisera. Lanes 'rec' were loaded with equimolar amounts of recombinant TEF and DBP. Positions of rat and recombinant proteins are indicated at the left and right. (**C**) Cellular TEF and DBP mRNA levels. The mRNA signals obtained in (A) have been quantified by scanning and are corrected for the following tissue-specific RNA:DNA ratios: 4.71 for liver, 1.41 for brain, 1.24 for kidney, 0.42 for spleen, 2.58 for testis and 0.56 for lung (Schmidt and Schibler, 1995a,b). The values are normalized to 1.0 respective to the liver p.m. value.

notable exception is brain, in which TEF is poorly expressed in spite of relatively high TEF mRNA levels.

TEF and DBP have different promoter preferences

Thus far, we have demonstrated that the two PAR proteins, DBP and TEF, exhibit similar tissue distributions and circadian accumulations. The question then arises as to whether these two proteins are functionally redundant. As a first attempt to elucidate this question, we examined the transactivation potential of DBP and TEF for two possible target promoters of PAR proteins. DBP was originally discovered as a transcription factor binding to a *cis*-acting element of the albumin promoter. Thereafter, it was suggested to be involved in the control of circadian transcription of the C7αH gene (Lavery and Schibler, 1993). Transcription of both the albumin and the C7αH genes cycles during the day, with a phase paralleling that of DBP and TEF accumulation. While the accumulation of C7αH is also circadian, albumin mRNA levels are similar throughout the day, probably because of the long half-life of albumin transcripts (Wuarin *et al.*, 1992; Lavery and Schibler, 1994). CAT reporter genes carrying either the albumin promoter (–170 to +22) or the C7αH promoter (–340 to +47) were co-transfected with TEF or DBP expression vectors. In order to compare directly the results obtained with these two transcription factors, the expression vector levels yielding similar nuclear concentrations for both TEF and DBP effector proteins in transfected cells were first evaluated. Figure 6A demonstrates that, at similar concentrations, DBP activates transcription from the C7αH promoter much more efficiently than does TEF. Indeed, even at the highest concentrations of TEF tested, C7αH reporter gene transcription was enhanced only 1.5-fold (data not shown). Conversely, TEF consistently exhibited an ~2-fold higher stimulation of transcription from the albumin promoter (25-fold activa-

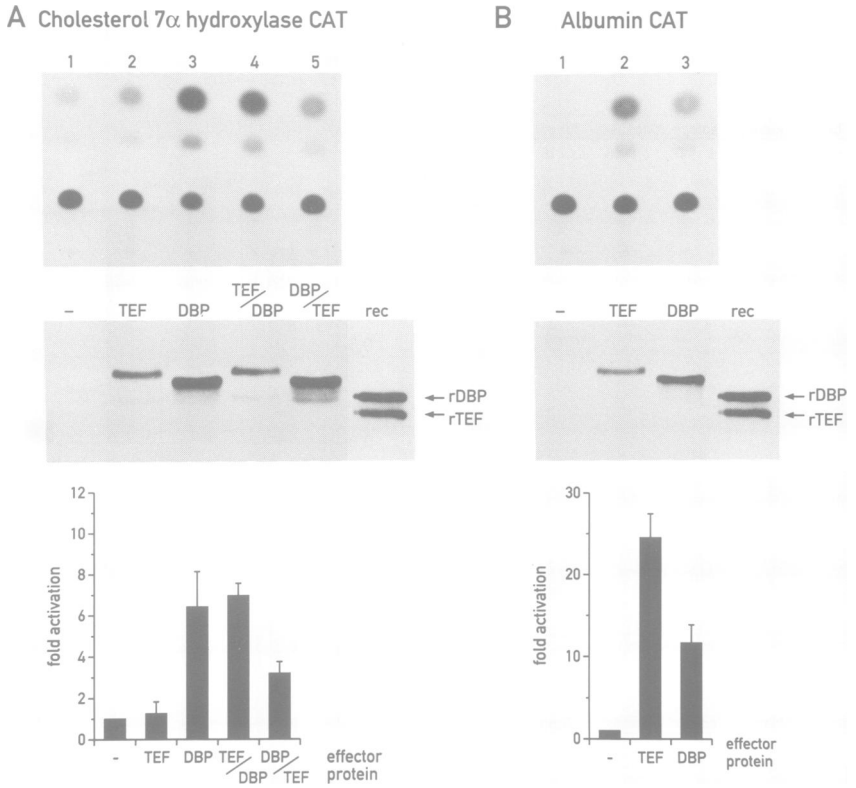

Fig. 6. Transcription activation from the C7αH and albumin promoters by TEF and DBP in co-transfected HepG2 cells. (**A**) Analysis of the C7αH promoter. Cells were transfected with 5 μg of C7αH–CAT alone, (lane 1), or C7αH–CAT (5 μg) with either 4 μg of CMV–TEF (lane 2), 2 μg of CMV–DBP (lane 3), 2 μg of CMV–TEF/DBP (lane 4) or 1 μg of CMV–DBP/TEF (lane 5). The upper panel shows the CAT assays obtained with extracts from transfected cells. The lower panel shows the Western blot analysis of nuclear lysates for the corresponding effector proteins using a crude DBP antiserum recognizing both DBP and TEF proteins. The 'rec' lane was loaded with an equimolar amount of recombinant TEF and DBP protein. The histogram shown in the bottom panel summarizes the relative TEF- and DBP-mediated transcription activations. Values were derived as described in Materials and methods and represent an average of three transfections. Error bars indicate standard deviations. (**B**) Similar representation of the albumin promoter analysis. Cells were transfected with 5 μg of albumin–CAT alone (lane 1), or albumin–CAT (5 μg) with either 2 μg of CMV–TEF (lane 2) or 2 μg of CMV–DBP (lane 3). The histogram shown in the bottom panel summarizes the relative TEF- and DBP-mediated transcription activations. Values represent an average of two transfections, error bars indicate standard deviations.

tion) than DBP (12-fold activation) (Figure 6B). At first, we suspected the least conserved N-terminal sequences of TEF and DBP to be responsible for their different promoter preferences. However, this assumption proved to be incorrect. When the bZip domains of TEF and DBP were exchanged, the protein harboring N-terminal TEF sequences fused to the DBP bZip region (TEF/DBP) activated C7αH reporter gene expression as well as DBP (Figure 6A, lane 4). The activity of the reciprocal fusion protein (DBP/TEF) in stimulating transcription from the C7αH promoter was intermediate between DBP and TEF (Figure 6A, lane 5).

Since most previous experiments revealing identical *in vitro* DNA binding specificity of PAR proteins were performed at 4°C (Falvey, Marcacci and Schibler, in preparation), we examined the possibility that the DNA binding specificity of TEF and DBP may differ at physiological temperature (37°C). Therefore, the equilibrium binding of these two proteins was compared at 4 and 37°C, using DNase I protection assays with purified recombinant proteins (Figure 7). While these measurements revealed considerably lower affinities for both proteins at the more elevated temperature, the relative affinities of TEF and DBP for the major PAR binding site (FP2) within the C7αH promoter did not differ dramatically at either temperature. In fact, at 37°C, TEF appears to bind FP2 ~2-fold more avidly than DBP. We also noted a subtle difference in the DNase I protection patterns observed with TEF or DBP. A DNase I-hypersensitive site (indicated by an arrow in Figure 7) observed with TEF and DBP at 4°C (Figure 7A) is detected only with TEF at 37°C (Figure 7B). As DNase I-hypersensitive sites are often suggestive of DNA bending (Brukner *et al.*, 1990), it is conceivable that TEF changes the path of its target DNA more dramatically than DBP at elevated temperatures.

Since TEF effectively stimulates transcription from the albumin–CAT, but not from the C7αH–CAT reporter gene, we examined whether conversion of the FP2 sequence to the albumin D site could rescue transcription activation of the C7αH promoter by TEF. The co-transfection experiments presented in Figure 8A suggest that this is not the case. Even conversion of FP2 into a perfect PAR consensus sequence (contained in the hamster PrP promoter, P.Fonjallaz, C.Weissmann and U.Schibler, unpublished results), which binds both PAR proteins with a 15-fold higher affinity than FP2 (compare Figure 7B and Figure 9), did not result in a significant activation of the C7αH

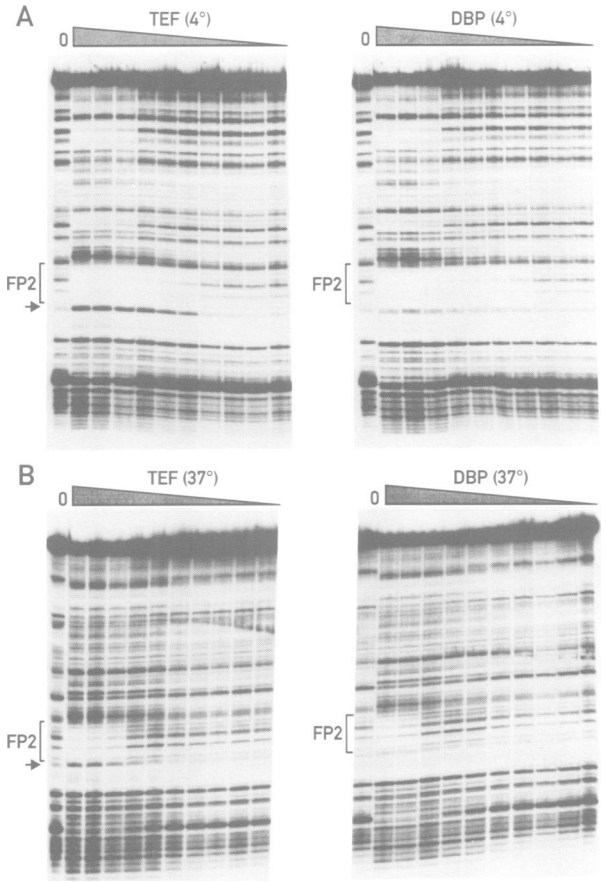

Fig. 7. Binding of TEF and DBP proteins to the C7αH promoter. (**A**) DNase I protection experiments performed at 4°C with recombinant short-TEF (left panel) or recombinant short-DBP (right panel), starting at a final concentration of 400 nM (monomers) and diluting it by 2-fold steps from left to right. '0' lanes indicate that no recombinant proteins were added to the reaction. Dissociation constants (K_ds) were estimated to be 6.25 nM (dimers) for both TEF and DBP (see Materials and methods). (**B**) Similar analysis performed at 37°C. Dissociation constants (K_ds) were estimated to be 100 nM (dimers) for TEF and 187 nM (dimers) for DBP (see Materials and methods). Brackets indicate the boundaries of the FP-2 site (Lavery and Schibler, 1993) and arrows denote DNase I-hypersensitive sites.

promoter by TEF (Figure 8B). It appears likely from these co-transfection experiments that the promoter environment, the geometry of the protein–DNA complex, or the binding dynamics, rather than the sequence of the actual PAR binding site, determine the promoter preferences of DBP and TEF.

We wished to examine whether TEF and DBP can be discriminated on the basis of their DNA binding dynamics (see Discussion). To this end, we used a UV-laser cross-linking approach (see Materials and methods) to measure the off-rate constants ($K_{off} = \ln 2/t_{1/2}$) of both proteins when bound to the perfect PrP PAR recognition sequence. As shown in Figure 9B, TEF–DNA and DBP–DNA complexes dissociate with similar half-lives (~110 s) and hence with similar off-rates (~6×10^{-3}/s). Since neither the equilibrium binding (K_d, for theoretical considerations, see Materials and methods), nor the off-rates of TEF and DBP differ drastically, the on-rate constant (K_{on}) must also be similar ($K_d = K_{off}/K_{on}$). This indicates that the overall binding dynamics are comparable for both proteins, when examined with the perfect PrP DNA consensus sequence.

Discussion

Tissue-specific and circadian regulation of TEF and DBP

Here we show that the expression of TEF and DBP, two members of the PAR family of bZip proteins, is similar with regard to tissue specificity and circadian rhythmicity. Among the tissues tested, both proteins reach their highest levels in liver, and are less concentrated in kidney and brain. DBP, but not TEF, can also be detected in lung nuclei, whereas neither of the two proteins accumulate to significant levels in spleen and testis. At first sight, there is little correlation between mRNA and protein accumulation in the six tissues examined (compare Figure 5A and B). However, with the exception of TEF accumulation in the brain, a large part of these apparent discrepancies can be explained by different average sizes of the cells constituting the various tissues (Schmidt and Schibler, 1995a,b). In the immunoblot experiments shown in Figure 5B, the proteins loaded onto the gel have been normalized to equal amounts of nuclear DNA and thus reflect cellular equivalents. In contrast, equal amounts of whole cell RNA have been used in the TEF and DBP mRNA analysis. Since large cells, such as parenchymal hepatocytes, contain more RNA than small cells, such as splenocytes or lung cells, the signals observed in RNase protection experiments have to be corrected for the tissue-specific RNA:DNA ratios in order to obtain the cellular equivalents of these mRNAs.

In liver and kidney (and lung for DBP), both TEF and DBP accumulate according to a stringent daily rhythm. For both proteins, maximal and minimal nuclear concentrations are reached at 8 p.m. and 8 a.m., respectively. These cycles are truly circadian, since they persist under free-running conditions, such as in constant dark or in the absence of food (Wuarin and Schibler, 1990; and this study). We thus suspect that the expression rhythms of both proteins are outputs of the circadian pacemaker that, in mammals, resides in the suprachiasmatic nucleus within the hypothalamus (for review, see Moore, 1992). It is thought that the hypothalamus–pituitary axis controls most outputs of the circadian clock. Several observations point towards a role of rhythmic glucocorticoid secretion in controlling circadian DBP expression in rat (Wuarin and Schibler, 1990; Wuarin *et al.*, 1992). Moreover, in the liver of transgenic mice with two mutant alleles for the glucocorticoid receptor, hepatic DBP mRNA levels are considerably lower than in wild-type mice (D.Lavery, T.Cole, G.Schuetz and U.Schibler, unpublished observations). Surprisingly, however, TEF mRNA expression seems to be less affected in these mutant mice. It is thus conceivable that not all of the systemic cues driving circadian DBP and TEF expression are shared.

While the cycle of DBP mRNA expression is sufficient to account for circadian DBP protein accumulation, this is not the case for TEF. In hepatocytes, the mRNA encoding this protein is only ~5- to 10-fold more concentrated in the evening than in the morning. Yet, TEF protein reaches ~50-fold higher nuclear concentrations at 8 p.m. than at 8 a.m. The 5- to 10-fold discrepancy between the circadian

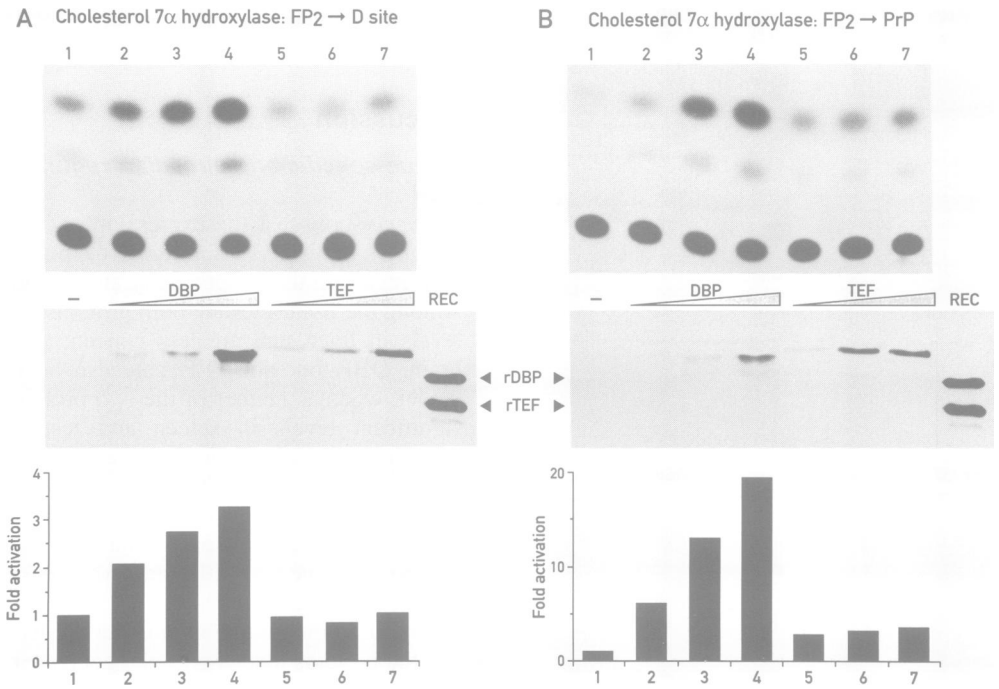

Fig. 8. Transcription activation from mutated C7αH promoters by TEF and DBP. Similar representation as in Figure 6. Analysis of a mutated C7αH promoter in which the FP-2 site has been converted into an albumin D element (**A**) or PrP element (**B**). Cells were transfected with 5 μg of mutated C7αH–CAT (lanes 1) alone; 5 μg of mutated C7αH–CAT with either 0.5 μg of CMV–DBP (lanes 2), 1 μg of CMV–DBP (lanes 3); 2 μg of CMV–DBP (lanes 4); 1 μg of CMV–TEF (lanes 5); 2 μg of CMV–TEF (lanes 6); or 4 μg of CMV–TEF (lanes 7).

amplitudes of TEF mRNA and protein accumulation could be caused by daily variations in: (i) TEF mRNA translation efficiency; (ii) TEF protein half-life and (iii) TEF nuclear translocation efficiency. As kinetic labeling studies are hardly feasible for rare proteins in the intact animal, in particular if their synthesis rate is not constant, we cannot distinguish incontrovertibly between these three mechanisms. However, the polysome distribution of TEF mRNA suggests that its translation rate does not vary dramatically during the day. One simple and attractive hypothesis would imply that TEF monomers decay faster than TEF dimers. At higher TEF mRNA concentrations (such as in the evening), correspondingly more TEF protein would be synthesized. As the proportion of monomers to dimers depends on the dimerization constant and the synthesis, this would drive the equilibrium towards dimers. As a consequence, proportionately more TEF molecules may decay at a lower degradation rate, characteristic for dimers, in the evening than in the morning. Thus, simply because the evening TEF synthesis rate (reflected by the TEF mRNA concentration) is 5- to 10-fold higher than the morning TEF synthesis rate, the average protein decay rate would be lower during the evening than during the morning. Since TEF can heterodimerize with DBP and HLF, which are also more abundant in the evening, the proportion of TEF molecules in dimers may be further increased during the evening. In this model, the decay rate varies as a function of synthesis rate, thus amplifying the differences in accumulation. Obviously, in this scenario, the amplification effect would be highest if, at minimal and maximal synthesis rates, most subunits were present as monomers and multimers, respectively. This may be the case for TEF but not for DBP, for which the daily variation of mRNA alone can account for a large part of the protein accumulation cycle.

Recently, the expression of HLF (Hunger *et al.*, 1992, 1994; Inaba *et al.*, 1992, 1994), the third gene of the PAR family, was also analyzed in detail (Falvey *et al.*, 1995). In rat, *hlf* is transcribed from two promoters, α and β, and specifies two transcriptional activator proteins with different N-terminal sequences, HLF43 and HLF36. Transcripts initiated at the α-promoter and their translation product, HLF43, accumulate in brain, liver and kidney, and in the latter two tissues are subject to stringent circadian control. In contrast, the levels of transcripts initiated at the β-promoter and the protein they encode, HLF36, vary only 3- and 2-fold, respectively, during the day. HLF36 is expressed predominantly in liver, and thus shows a more restricted tissue distribution than HLF43. Interestingly, the phase of circadian HLF43 and HLF36 oscillation is delayed by ~4 h with regard to DBP and TEF. Conceivably, the two HLF proteins may activate genes whose products are required at a later time during the day than those regulated by DBP and TEF.

All three PAR family genes are located on different chromosomes. In man, DBP, TEF and HLF have been assigned to chromosomes 19q13, 22q13 (Khatib *et al.*, 1994) and 17q22 (Inaba *et al.*, 1992) respectively. Therefore, the similar expression pattern of these three genes with regard to tissue specificity and circadian rhythmicity cannot be controlled from common *cis*-acting regulatory sequences, such as described for genes of the β-globin locus (Dillon and Grosveld, 1993). However, it is conceivable, if not likely, that the PAR family gene promoters and enhancers share some *cis*-acting elements interacting with the same transcriptional regulatory proteins. The

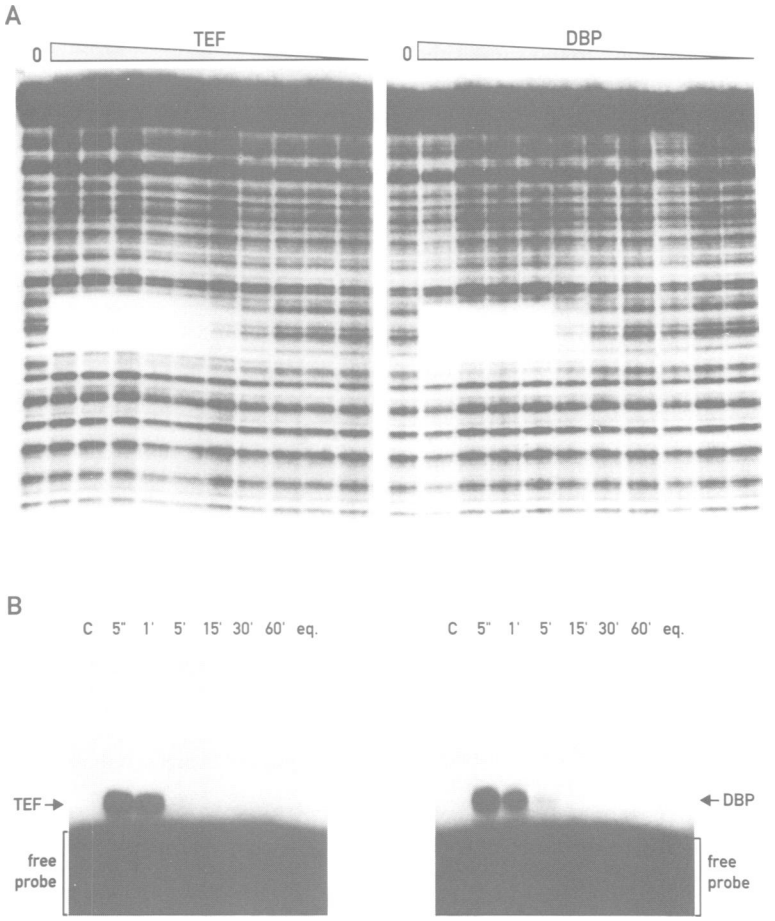

Fig. 9. Binding of TEF and DBP proteins to the high affinity PrP recognition sequence at 37°C. (**A**) Equilibrium binding. The same conditions and protein concentrations were used as in Figure 7B, except that an end-labeled PrP promoter fragment encompassing a high affinity PAR recognition sequence centered around –230 was used. Dissociation constants (K_ds) were estimated to be 6.25 nM (dimers) for TEF and 12.5 nM (dimers) for DBP (see Materials and methods). (**B**) Off-rate constants for TEF and DBP. UV-laser cross-linking experiments (see Materials and methods) were used to estimate the dissociation off-rates of TEF and DBP from the PrP PAR recognition site at 37°C. Numbers above each lane denote time elapsed between unlabeled binding site addition and UV-laser cross-linking. Lane 'C' indicates that no recombinant protein was added to the reaction. Lane 'eq' indicates competition equilibrium; in this reaction both the labeled and unlabeled recognition sites were pre-mixed prior to the addition of recombinant proteins. The positions of cross-linked protein–DNA complexes containing TEF or DBP, as well as the position of the unbound probe, are depicted at the left and right of each panel. The half-lives of the TEF–DNA and DBP–DNA complexes have been estimated to be 110 s for both proteins. Given that off-rates are equivalent to $\ln 2/t_{1/2}$, the off-rates for TEF and DBP were estimated to be 6.3×10^{-3}/s for both proteins.

promoter regions of all three genes have been cloned and studies are underway to examine this possibility.

TEF and DBP have different promoter preferences

In vitro, TEF, HLF and DBP recognize the same DNA sequences (Drolet *et al.*, 1991; Falvey *et al.*, 1995; this study). Moreover, as discussed in the previous section, all three of these proteins are co-expressed in several organs, and their accumulation follows a circadian rhythm. This begs the question of whether PAR proteins are functionally equivalent. For two reasons, we consider this to be unlikely. First, the amino acid sequences that differ between the three PAR proteins were highly conserved during evolution (see Introduction), a finding that is difficult to reconcile with functional redundancy. Second, and more importantly, in the co-transfection experiments presented here, DBP and TEF have different activation potentials for the albumin and the C7αH promoter, two putative target promoters of PAR proteins. These functional differences are remarkable, considering that, in transfected cells, effector proteins may reach much higher concentrations than those observed in normal tissues. According to mass action law, overexpression of transcription factors is likely to attenuate differences observed at limiting concentrations of regulatory proteins. Unexpectedly, the different transactivation capacity of TEF and DBP for the C7αH promoters could be attributed largely to the conserved bZip regions of the two proteins. Moreover, even conversion of FP2 into a perfect PAR protein binding consensus sequence with an ~15-fold higher affinity does not improve TEF-mediated transcription activation from the C7αH promoter. It is thus conceivable that the bZip regions of PAR proteins mediate promoter-specific activation by a mechanism which does not implicate DNA binding equilibrium as a rate-limiting parameter.

We considered the possibility that binding kinetics, rather than the binding equilibrium, may differ for DBP and TEF. The binding dynamics may be important in a scenario of kinetic synergism (Herschlag and Johnson, 1993). For example, if different proteins with affinity for

the PAR recognition sequence, such as PAR and C/EBP proteins, would have to bind sequentially to the same site, thereby enhancing rate constants for different initiation events, a protein with low on- and off-rates may be a less potent activator than a protein with high on- and off-rates. However, we estimated the off-rates for DBP and TEF from the high affinity PAR recognition site of the PrP promoter to be similar. Thus, at least for the mutagenized C7αH promoter carrying the PrP element (Figure 8B), differences in binding dynamics are unlikely to account for the different activation potentials of DBP and TEF. Why can TEF not stimulate transcription from the C7αH promoter even though its N-terminal activation domain is fully functional when provided with a DBP bZip region? Conceivably, the geometry of the TEF–DNA complex, unlike the DBP–DNA complex, is incompatible with C7αH transcription activation. In this context, it may be noteworthy that, at 37°C, hypersensitive sites, suggestive of DNA bending (Brukner *et al.*, 1990) have been discerned in DNase I protection experiments of this promoter region with TEF but not with DBP. Further experiments are required to elucidate the subtle binding differences in TEF and DBP, and their significance for transcription activation.

Different transactivation potentials for the C7αH promoter and the albumin promoter have also been described for HLF43 and HLF36 (Falvey *et al.*, 1995). HLF43 is a very potent activator of the C7αH promoter and a poor activator for the albumin promoter, while the opposite holds true for HLF36. The only difference between these two proteins is that HLF43 possesses an extra N-terminal amino acid segment of 49 amino acids. Thus, HLF proteins are not functionally distinct for the same reason as DBP and TEF. Rather, the difference of HLF43 and HLF36 may be accounted for by different contacts that their N-terminal sequences establish with other components of the transcription machinery. The family of PAR bZip proteins may thus become a paradigm for how subtle differences in protein–DNA and/or protein–protein interactions may lead to different specificities of transcriptional regulatory proteins.

Materials and methods

Plasmid construction

The eukaryotic and bacterial TEF expression plasmids were generous gifts from Daniel Drolet and Jeff Rosenfeld (Drolet *et al.*, 1991). The plasmids CMV–DBP, albumin–CAT (Mueller *et al.*, 1990) and –340 C7αH–CAT (Lavery and Schibler, 1993) have been described previously. The mammalian expression plasmid CMV–TEF/DBP (for the structure of the CMV expression vector, see Rusconi *et al.*, 1990) encodes a fusion protein containing TEF residues 1–217 (N-terminal and PAR domain) linked to DBP residues 240–325 (basic and leucine zipper domain). Similarly CMV–DBP/TEF encodes a fusion protein containing DBP residues 1–238 linked to TEF residues 217–301. DNA sequences encoding junctions of these fusion protein expression plasmids were sequenced, and the proteins produced in transfected cells were analyzed by immunoblotting and gel retardation assays. The pET3 bacterial expression plasmids encoding short-TEF and short-DBP contain coding sequences spanning the PAR, basic and leucine zipper regions (residues 152–261 for short-TEF and residue 211–325 for short-DBP). Recombinant proteins were overproduced and purified on heparin–agarose columns as described previously (Descombes *et al.*, 1990). C7αH promoter mutants with modified PAR recognition sequences were constructed by site-directed mutagenesis, converting the wild-type FP-2 site GTTATGTCAG (Lavery and Schibler, 1993) either into an albumin D element ATTTTGTAAT or the perfect PAR consensus sequence ATTATGTAAC found in the PrP promoter (Basler *et al.*, 1986). The plasmid pKS+PrP was obtained by subcloning a *Taq*I–*Rsa*I fragment from SPrP 7.1 (generous gift from C.Weissmann) into the *Sma*I site of pKS+ (Stratagene). pKS+TEF95 and pKS+DBP95 contain 95 bp PCR products spanning the basic and leucine zipper domain of TEF (position 598–693) and DBP (position 1126–1221), respectively, cloned into the *Eco*RV site of pKS+.

DNase I footprint experiments

DNase I footprinting was performed as described (Lichtsteiner *et al.*, 1987), using a *Hin*dIII–*Alw*44I C7αH promoter fragment (Lavery and Schibler, 1993) labeled at the *Hin*dIII site with *E.coli* DNA polymerase I (Klenow fragment) and [α-^{32}P]dATP, or a *Bam*HI–*Pst*I PrP promoter fragment (from pKS+PrP), labeled at the *Bam*HI site with Klenow DNA polymerase. Radiolabeled DNAs (1 nM final concentration, ~10 000 c.p.m.) were incubated with serial dilutions of recombinant short-TEF or short-DBP proteins (0.8–400 nM final concentration, see legend to Figure 7). Samples were then digested for 1 min with DNase I (Boehringer, 10 μg/ml on ice, 33.33 ng/ml at 37°C). Digestions were stopped by the addition of EDTA to 20 mM and SDS to 0.5%, and DNA was purified by phenol–chloroform extraction and ethanol precipitation. DNA fragments were displayed on a 6% polyacrylamide–8 M urea sequencing gel. If in all reactions the protein is in excess over the DNA, and if the dimerization equilibrium constants of PAR proteins are below the concentrations required for DNA binding (for PAR protein dimerization constants, see Krylov *et al.*, 1994), the concentration of free protein dimers approaches $[P_0]/2$ (P_0 = total protein concentration). Thus, the equilibrium constant can be written as $K_d = [P_0/2]\cdot[D]/[PD]$, where [PD] is the concentration of the protein–DNA complex, and [D] is the concentration of free DNA. At half saturation of the DNA, [PD] is equal to [D], therefore the K_d corresponds to the protein concentration $[P_0/2]$ required to occupy half of the DNA molecules.

Off-rate determinations

Off-rates (K_{off}) for TEF and DBP were estimated by using a UV-laser cross-linking assay. Short-TEF or short-DBP recombinant proteins (10 nM final concentration) and a labeled oligonucleotide harboring the PrP PAR recognition sequence (1 nM final concentration) were incubated at 37°C for 15 min to allow protein–DNA binding to reach equilibrium. Binding to the radiolabeled recognition sequence was then competed by adding a 660-fold excess of unlabeled oligonucleotide (660 nM final concentration). Aliquots (50 μl) were irradiated after different time periods by a UV-laser pulse (Spectra-Physics Quanta-Ray GCR Series laser, 5 ns pulse at 266 nm), thereby photo-cross-linking a constant proportion of the protein–DNA complex. Covalent protein–DNA complexes were separated from free DNA by SDS–PAGE. The relative radioactivities associated with the protein–DNA complexes were quantified by using a PhosphorImager (Bio-Rad GS-250).

RNA isolation and analysis

Whole cell RNA was isolated from different rat tissues as described previously (Schmidt and Schibler, 1995a). For Northern blot analysis, polyadenylated liver RNA was selected from whole cell RNA by two rounds of oligo(dT)–cellulose chromatography. RNA was separated on a 1.5% agarose gel containing 0.6 M formaldehyde, transferred onto Nytran membrane (Schleicher and Schuell) and hybridized to an antisense RNA probe transcribed from pKS+TEF95, linearized by digestion with *Hin*dIII. Hybridization and washing conditions were carried out as previously described (Falvey *et al.*, 1995). RNase protection analysis was performed with 50 μg of whole cell RNA, as described previously (Schmidt and Schibler, 1995a), using antisense probes. The TEF antisense RNA probe was obtained by *in vitro* transcription of *Hin*dIII-digested pKS+TEF95 (see above) with T7 RNA polymerase, while the DBP probe was obtained by transcribing *Eco*RI-digested pKS+DBP95 (see above) with T3 RNA polymerase (P.F., unpublished). The GAPDH antisense probe was prepared as described previously (Schmidt and Schibler, 1995a). Signals were quantified using a Bio-Rad GS-250 PhosphorImager. Polysome fractionation and analysis of polysome-associated RNA by RNase protection, using the TEF-specific antisense probe (see above), were performed as previously described (Schmidt and Schibler, 1995a).

Isolation of nuclei and protein extraction

Nuclei were purified from rat tissues as described previously (Tian and Schibler, 1991), resuspended in nuclear storage buffer [20 mM Tris–Cl (pH 7.9), 75 mM NaCl, 0.5 mM EDTA, 0.85 mM dithiothreitol (DTT), 0.125 mM phenylmethylsulfonyl fluoride (PMSF), 20% glycerol] and,

after the DNA content of the suspension had been determined spectrophotometrically, the nuclei were frozen in liquid nitrogen and stored at –70°C.

Extraction of nuclear proteins was performed according to the NUN protocol described previously (Lavery and Schibler, 1993).

Preparation and purification of monospecific antibodies

Rabbit anti-TEF antibodies were raised according to standard procedures (Harlow and Lane, 1988) against a recombinant protein encoded by the *E.coli* expression vector pET3 rat TEF (Drolet *et al.*, 1991), purified by heparin–agarose column chromatography. Antibodies cross-reacting with DBP and HLF were eliminated from the crude rabbit antiserum by first passing it over an Affigel-10 column (Bio-Rad) coupled to recombinant full-length DBP and then over an Affigel-10 column coupled to recombinant full-length HLF. TEF-specific antibodies were then obtained from the final flowthrough by affinity purification on an Affigel-10 column containing recombinant TEF. A similar immunodepletion procedure was applied to DBP antisera, but the final affinity purification against immobilized DBP was omitted, since the immunodepleted antiserum did not produce a high background in Western blot experiments.

Western blot analysis

Immunochemical detection of TEF and DBP proteins in nuclear lysates was performed using the respective purified antisera (described above) at a final dilution of 1:100 (TEF) or 1:1000 (DBP), as described (Wuarin and Schibler, 1990). Approximately 25 μg of nuclear proteins were analyzed in immunoblot experiments. An equimolar mixture of TEF and DBP recombinant proteins was analyzed along with nuclear proteins to control for antisera specificity. Immune complexes were detected using a peroxidase-conjugated secondary antibody (Jackson Immunoresearch Laboratories) and the ECL detection kit (Amersham), according to the manufacturer's specifications.

Transient transfection assays

HepG2 cells were transiently transfected by the calcium phosphate coprecipitation procedure as previously described (Mueller *et al.*, 1990) with the indicated amount of expression vector. All transfections contained a total of 15 μg/9 cm plate, including 5 μg of the CAT reporter gene, 2 μg of an RSV luciferase vector and the indicated amounts of DBP or TEF expression vectors supplemented to 15 μg with pKS+. Isolation of nuclear extracts for Western blot analysis of effector proteins and cellular extracts for the CAT assays were performed as previously described (Descombes and Schibler, 1991). CAT activity was assayed by standard methods (Gorman *et al.*, 1982), and the proportion of acetylated chloramphenicol was estimated by scanning the thin layer chromatography plates using a Berthold TLC linear analyzer. Values were normalized for transfection efficiency by assaying luciferase activity with a Bio-Orbit luminometer. The value of 'fold activation' was obtained by dividing the corrected CAT value by the background level obtained with the CAT reporter gene alone.

Mathematical simulations

Data points for TEF and DBP mRNA oscillation were obtained by densitometric scanning of the RNase protection experiment presented in Figure 2B using the Shimadzu CS-9000 dual wavelength flying spot scanner. Data points for TEF and DBP protein oscillations were determined similarly by densitometric scanning of the Western blot experiment shown in Figure 1A. Curve-fitting and simulation were obtained as follows: in a first step, we searched for an analytic expression for $f(t)$ of TEF or DBP mRNA in the form of a shifted and periodically repeated Gaussian curve:

$$f(t) = \alpha \sum_{k=-\infty}^{k=+\infty} e^{-(t-\beta-24k)^2/\gamma}$$

The free parameters α, β, γ were adjusted to the experimentally determined mRNA values by a non-linear Gauss–Newton algorithm (Deuflhard and Hohmann, 1991). In a second step, parameter C and $t_{1/2}$ in the integral (Equation 1) (see text) were adjusted to the experimental protein accumulation data points. This was done by using the above mentioned Gauss–Newton algorithm. Thereby, at each function call with given parameter values, the integral (Equation 1) was computed by solving its corresponding differential equation $dP/dx = C \cdot f(x) - \ln 2/t_{1/2} \cdot P(x)$ with periodic boundary conditions using the Runge–Kutta code DoPRI5 (Hairer *et al.*, 1993).

Acknowledgements

We are grateful to D.Drolet and M.G.Rosenfeld for generous gifts of various TEF plasmids, and C.Weissmann for a plasmid harboring hamster PrP promoter sequences. We thank H.Geiselmann for his advice in the UV-laser photo-cross-linking experiments, and D.Lavery and E.Schmidt for their critical reading of the the manuscript. Ed Schmidt's help in polysome gradient analysis is highly appreciated. This work was supported by the state of Geneva, and by grants of the Swiss National Science Foundation to U.S. (31-31028-91) and G.W. (20-40665.94).

References

Basler,K., Oesch,B., Scott,M., Westaway,D., Waechli,M., Groth,D.F., McKinley,M.P., Prusiner,S.B. and Weissman,C. (1986) Scrapie and cellular PrP isoforms are encoded by the same chromosomal gene. *Cell*, **46**, 417–428.

Brukner,I., Jurukowski,V. and Savic,A. (1990) Sequence-dependent structural variation of DNA revealed by DNase I. *Nucleic Acids Res.*, **18**, 891–894.

Burch,J.B.E. and Davis,D.L. (1994) Alternative promoter usage and splicing options result in the differential expression of mRNAs encoding four isoforms of chicken VBP, a member of the PAR subfamily of bZIP transcription factors. *Nucleic Acids Res.*, **22**, 4733–4741.

Cao,Z., Umek,R.M. and McKnight,S.L. (1991) Regulated expression of three C/EBP isoforms during adipose conversion of 3T3-L1 cells. *Genes Dev.*, **5**, 1538–1552.

Descombes,P. and Schibler,U. (1991) A liver-enriched transcriptional activator protein, LAP, and a transcriptional inhibitory protein, LIP are translated from the same mRNA. *Cell*, **67**, 569–579.

Descombes,P., Chojkier,M., Lichtsteiner,S., Falvey,E. and Schibler,U. (1990) LAP, a novel member of the C/EBP gene family, encodes a liver-enriched transcriptional activator protein. *Genes Dev.*, **4**, 1541–1551.

Deuflhard,P. and Hohmann,A. (1991) *Numerische Mathematik*. Walter de Gruyter, Berlin/New York.

Dillon,N. and Grosveld,F. (1993) Transcriptional regulation of multigene loci: multilevel control. *Trends Genet.*, **9**, 134–137.

Drolet,D.W., Scully,K.M., Simmons,D.M., Wegner,M., Chu,K., Swanson,L.W. and Rosenfeld,M.G. (1991) TEF, a transcription factor expressed specifically in the anterior pituitary during embryogenesis, defines a new class of leucine zipper proteins. *Genes Dev.*, **5**, 1739–1753.

Falvey,E., Fleury-Olela,F. and Schibler,U. (1995) The rat hepatic leukemia factor (HLF) gene encodes two transcriptional activators with distinct circadian rhythms, tissue distribution and target preferences. *EMBO J.*, **14**, 4307–4317.

Gorman,C.M., Moffat,L.F. and Howard,B.H. (1982) Recombinant genomes which express chloramphenicol acetyltransferase in mammalian cells. *Mol. Cell. Biol.*, **2**, 1044–1051.

Haas,N.B., Cantwell,C.A., Johnson,P.F. and Burch,J.B.E. (1995) DNA-binding specificity of the PAR basic leucine zipper protein VBP partially overlaps those of the C/EBP and CREB/ATF families and is influenced by domains that flank the core basic region. *Mol. Cell. Biol.*, **15**, 1923–1932.

Hairer,E., Hohmann,A. and Wanner,G. (1993) *Solving Ordinary Differential Equations I*. 2nd edn, Springer-Verlag, SCM8.

Harlow,E. and Lane,D. (1988) *Antibodies: A Laboratory Manual*. Cold Spring Harbor Laboratory Press, Cold Spring Harbor, NY.

Herschlag,D. and Johnson,F.B. (1993) Synergism in transcriptional activation: a kinetic view. *Genes Dev.*, **7**, 173–179.

Hunger,S.P., Ohyashiki,K., Toyama,K. and Cleary,M.L. (1992) HLF, a novel hepatic bZIP protein, shows altered DNA-binding properties following fusion to E2A in t(17;19) acute lymphoblastic leukemia. *Genes Dev.*, **6**, 1608–1620.

Hunger,S.P., Brown,R. and Cleary,M.L. (1994) DNA-binding and transcriptional regulatory properties of hepatic leukemia factor (HLF) and the t(17;19) acute lymphoblatic leukemia chimera E2A-HLF. *Mol. Cell. Biol.*, **14**, 5986–5996.

Inaba,T., Roberts,W.M., Shapiro,L.H., Jolly,K.W., Raimondi,S.C., Smith,S.D. and Look,A.T. (1992) Fusion of the leucine zipper gene HLF to E2A gene in human acute B-lineage leukemia. *Science*, **257**, 531–534.

Inaba,T., Shapiro,L.H., Funabiki,T., Sinclair,A.E., Jones,B.G., Ashmun,R.A. and Look,A.T. (1994) DNA binding specificity and

transcriptional potential of the leukemia associated E2A–hepatic leukemia factor fusion protein. *Mol. Cell. Biol.*, **14**, 3403–3413.

Iyer,S.V., Davis,D.L, Seal,S.N. and Burch,J.B.E. (1991) Chicken vitellogenin gene-binding protein, a leucine zipper transcription factor that binds to an important control element in the chicken vitellogenin II promoter, is related to rat DBP. *Mol. Cell. Biol.*, **11**, 4863–4875.

Khatib,Z.A., Inaba,T., Valentine,M. and Look,A.T. (1994) Chromosomal localization and cDNA cloning of the human DBP and TEF genes. *Genomics*, **23**, 344–351.

Krylov,D., Mikhailenko,I. and Vinson,C. (1994) A thermodynamic scale for leucine zipper stability and dimerization specificity: e and g interhelical interactions. *EMBO J.*, **13**, 2849–2861.

Lavery,D.J. and Schibler,U. (1993) Circadian transcription of the cholesterol 7α hydroxylase gene may involve the liver-enriched bZIP protein DBP. *Genes Dev.*, **7**, 1871–1884.

Lavery,D.J. and Schibler,U. (1994) DBP and related transcription factors of the PAR family. In Tronche,F. and Yaniv,M. (eds), *Liver Gene Expression*. Molecular Biology Intelligence Unit, R.G.Landes Company, Austin, TX, pp. 259–275.

Lichtsteiner,S., Wuarin,J. and Schibler,U. (1987) The interplay of DNA-binding proteins on the promoter of the mouse albumin gene. *Cell*, **51**, 963–973.

Moore,R.Y. (1992) The suprachiasmatic nucleus and the circadian timing system. *Disc. Neurosci.*, **8**, 26–32.

Mueller,C.R., Maire,P. and Schibler,U. (1990) DBP, a liver-enriched transcriptional activator, is expressed late in ontogeny and its tissue-specificity is determined posttranscriptonally. *Cell*, **61**, 279–291.

Rusconi,S., Severne,Y., Georgiev,O., Galli,I. and Wieland,S. (1990) A novel expression assay to study transcriptional activators. *Gene*, **89**, 211–221.

Schmidt,E.E. and Schibler,U. (1995a) Cell size regulation, a mechanism that controls cellular RNA accumulation: consequences on regulation of the ubiquitous transcription factors Oct1 and NF-Y, and the liver-enriched transcription factor DBP. *J. Cell Biol.*, **128**, 467–483.

Schmidt,E.E. and Schibler,U. (1995b) High accumulation of components of the RNA polymerase II transcription machinery in rodent spermatids. *Development*, **121**, 2373–2383.

Tian,J.M. and Schibler,U. (1991) Tissue-specific expression of the gene encoding hepatocyte nuclear factor 1 may involve hepatocyte nuclear factor 4. *Genes Dev.*, **5**, 2225–2234.

Wuarin,J. and Schibler,U. (1990) Expression of the liver-enriched transcriptional activator protein DBP follows a stringent circadian rhythm. *Cell*, **63**, 1257–1266.

Wuarin,J., and Schibler,U. (1994) Physical isolation of nascent RNA chains transcribed by RNA polymerase II: evidence for cotranscriptional splicing. *Mol. Cell. Biol.*, **14**, 7219–7225.

Wuarin,J., Falvey,E., Lavery,D.J., Talbot,D., Schmidt,E.E., Ossipow,V., Fonjallaz,P. and Schibler,U. (1992) The role of the transcriptional activator protein DBP in circadian liver gene expression. *J. Cell Sci.* (Suppl.), **16**, 123–127.

Received on August 18, 1995; revised on September 29, 1995